Slotoxin, αKTx1.11, a new scorpion peptide blocker of MaxiK channels that differentiates between α and α+β (β1 or β4) complexes

Jesus Garcia-Valdes[a,1], Fernando Z. Zamudio[a], Ligia Toro[b], Lourival D. Possan[a,*]

[a] *Department of Molecular Recognition and Structural Biology, Institute of Biotechnology, National Autonomous University of Mexico, Avenida Universidad 2001, P.O. Box 510-3, Cuernavaca 62210, Mexico*
[b] *Departments of Anesthesiology and Molecular and Medical Pharmacology, Brain Research Institute, University of California, Los Angeles, CA 90095-7115, USA*

Received 13 July 2001; accepted 26 July 2001

First published online 5 September 2001

Edited by Maurice Montal

Abstract A novel peptide from *Centruroides noxius* Hoffmann scorpion venom was isolated and sequenced. The 37 amino acid peptide belongs to the charybdotoxin sub-family (αKTx1) and was numbered member 11. αKTx1.11 has 75% sequence identity with iberiotoxin and 54% with charybdotoxin. αKTx1.11 revealed specificity for mammalian MaxiK channels (hSlo), thus, was named slotoxin. Slotoxin blocks the MaxiK pore-forming α subunit reversibly (K_d = 1.5 nM). Slotoxin association with α+β (β1 or β4) channels was ~10 times slower than iberiotoxin and charybdotoxin, leading to a lack of effect on α+β4 when tested at 100 nM for 5 min. Thus, slotoxin is a better tool to distinguish MaxiK α+β complexes.

Key words: BK channel; Scorpion toxin; Pharmacology; Potassium channel; *Centruroides noxius*

1. Introduction

The large-conductance voltage and calcium-activated potassium (MaxiK, BK) channels are intrinsic membrane proteins that regulate excitability in a large variety of tissues including brain and smooth muscle [1]. MaxiK can be formed only by α subunits or by complexes with at least four families of β subunits [2–5]. The α subunit (Slo) is formed by the 'core' that includes transmembrane segments S0–S6 and hydrophobic regions S7–S8, the C-terminal 'tail' containing S9–S10, and the linker that binds both domains [6]. The 'core' contains the voltage sensor, the pore region and the site for β1 subunit interaction [7–9]. The pore is formed by the loops of amino acid sequences between the fifth and sixth membrane spanning domains, and is the place where permeation of ions occur, and where many pharmacologically active peptides bind [10]. Co-expression with β subunits (with two transmembrane domains and a large extracellular loop) modifies the MaxiK α-subunit kinetic behavior, Ca^{2+} sensitivity, modulation, and pharmacological properties like scorpion toxin sensitivity [5,11–15].

Scorpion venoms are rich sources of peptides, which have a variety of pharmacological effects on ion channels. Of special interest are those that affect ionic membrane permeability [10,16] as they have been excellent tools to study ion channel function and structure [17]. About 50 different peptides from scorpion venoms were recently revised and classified within 12 sub-families, based mainly on structural similarities [18]. All of these peptides have between 23 and 42 amino acid residues. They have in common an α-helix, two or three anti-parallel β-sheets, and three or four disulfide bridges that shape the three-dimensional structure and are essential for channel recognition [19]. Most scorpion toxins specific for K^+ channels are known to behave as pore blockers. The affinity of a given toxin for different types or sub-types of K^+ channels can vary several orders of magnitude [16,17].

Here we describe a new scorpion toxin αKTx1.11 (slotoxin (SloTx)) that specifically inhibits mammalian MaxiK channels and is capable of differentiating among three types of complexes, α, α+β1 and α+β4.

2. Materials and methods

2.1. Chemicals, venom and purification procedure

All chemicals were analytical grade reagents obtained from sources already described [20,21]. Scorpions of the species *Centruroides noxius* were milked for venom in the laboratory. The crude venom was dissolved in distilled water and spun at 10 000×*g* for 15 min. The supernatant was separated by column (0.9×190 cm) Sephadex G-50 gel filtration, followed by high-performance liquid chromatography (HPLC) using a semi-preparative C_{18} reverse-phase column (Vydac, Hisperia). Several independent runs of HPLC were obtained. The active fraction was further separated in an analytical C_{18} reverse-phase column using a different gradient (see legend to Fig. 1).

2.2. Amino acid sequence

The amino acid sequence was obtained by automatic Edman degradation in a LF3000 Protein Sequencer (Beckman) [20]. Samples of approximately 1 nmol each of native toxin or reduced and alkylated toxin were applied to the sequencer. A sample of peptide was also cleaved by cyanogen bromide (CNBr) after N-terminal blockade and sequenced. The last amino acid was elucidated by mass spectrometry analysis. The molecular masses were obtained on a Voyager DE-PRO (PerSeptive Biosystems) equipped with a nitrogen laser (337 nm) [22].

2.3. Electrostatic potential analysis

Electrostatic potentials were obtained after homology modeling and energy minimization using parameters of charybdotoxin (ChTx) solution structure (Swiss-Prot Accession No. 2CRD), Swiss-Model and Deep View (Swiss-Pdb Viewer) [23] (http://www.expasy.ch/spdv/).

2.4. Electrophysiological measurements

cRNA for hSlo (human MaxiK α subunit), dSlo (*Drosophila* MaxiK α subunit), Herg, IRK, Kv1.1, ShIR, SK1, SK2 and SK3 α sub-

*Corresponding author. Fax: (52)-73-172388.
E-mail address: possani@ibt.unam.mx (L.D. Possan).

[1] Present address: Department of Anesthesiology, University of California, Los Angeles, CA 90095-7115, USA.

0014-5793/01/$20.00
PII: S0014-5793(01)02791-0

units and MaxiK β1 and β4 subunits were synthesized using mMESSAGE mMACHINE In Vitro Transcription Kit (Ambion). cRNA were injected into *Xenopus* oocytes using 1–2 ng of α subunits, and when appropriate, with ~20-fold molar excess of β subunits. These conditions have shown a saturating effect of the β subunit on the Ca^{2+}-sensitivity of MaxiK α subunit [4,13]. Potassium currents were recorded 2–7 days after RNA injection.

2.4.1. Two-electrode voltage-clamp. The bath solution was ND-96 (mM): 96 NaCl, 2 KCl, 1.8 $CaCl_2$, 1 $MgCl_2$, 5 HEPES, pH 7.0, with NaOH, or modified ND-96 (containing 30 mM KCl and 68 NaCl). Resistance for the voltage and current electrodes were 0.3–0.5 and 1.0–1.5 MΩ, respectively, when filled with 3 M KCl. Holding potentials were: −90 mV for Herg, −80 mV for ShIR and Kv1.1, and 0 mV for IRK2.1. Pulses were from −80 to +80 in 10 mV steps. For Herg, post-test potential was to −120 mV. Macroscopic currents were recorded using the CA1B amplifier (Dagan Corporation). Currents were filtered at 1/5 of the sampling frequency.

2.4.2. Outside-out patches. Pipet and bath solutions contained (mM): 110 K-methanesulfonate, 5 KCl, 10 HEPES, 5 N-(2-hydroxyethyl)ethyl-enediaminetriacetic acid, pH 7.0. Different free intracellular Ca^{2+} solutions were prepared by addition of $CaCl_2$ according to the Chelator program [24] and adjusted using a calcium-selective electrode (World Precision Instruments). Patch pipets had resistances of 2–4 MΩ. Holding potential was 0 mV for dSlo, hSlo, SK1, SK2 and SK3. An EPC-7 amplifier (List Medical) and pCLAMP software (Axon Instruments) were used for acquisition and analysis. Bovine serum albumin (0.001%) was present in all toxin and washing solutions.

2.4.3. Curve fitting. Pharmacological experiments were fitted assuming a bimolecular reaction. Association (k_{on}) and dissociation (k_{off}) rates, and equilibrium dissociation constants (K_d) were obtained as described before [5]. Values are mean ± S.D.

3. Results and discussion

3.1. Isolation and characterization of the new toxin, αKTx1.11

Three distinct fractions (Fig. 1a, I, II and III) were obtained after separation of *C. noxius* soluble venom on a Sephadex G-50 column. Only fraction II was capable of inhibiting MaxiK currents assayed at 30 μg/ml protein. Fraction II was further purified by HPLC in a C_{18} semi-preparative column yielding a complicated pattern of separation (Fig. 1b). To facilitate identification of active peptides, the HPLC output was pooled into six fractions II.1 to II.6 (horizontal bars, labeled 1 to 6). Only fraction II.2 blocked MaxiK currents ($n = 3$). This fraction contained about 22 different components (Fig. 1b, left-side inset), but only component 22 had MaxiK channel activity ($n = 3$). Therefore, component number 22 (asterisk) was further purified to homogeneity (Fig. 1b, right-side inset).

The purified peptide was directly sequenced and the first 36 amino acid residues were unequivocally identified (Fig. 1c, arrow marked with d). The presence of a Met in position 29 facilitated CNBr cleavage of the peptide. The N-terminal amino acid was alkylated before CNBr cleavage. Sequence determination of the C-terminal peptide confirmed the sequence of the last seven residues (Fig. 1c, arrow marked with CNBr). The last residue was obtained by mass spectrometry analysis (Fig. 1c, arrowhead marked with MS). The native peptide had a molecular mass of 4082.82. The first 36 residues accounted for a mass of 3983.83, taking into consideration the three disulfide bridges typical of MaxiK blocking toxins [19]. The missing amino acid residue of the sequence should have a molecular mass of 99.01, which corresponds exactly to that of valine. Thus, it is very likely that the full amino acid sequence of this peptide contains 37 amino acid residues.

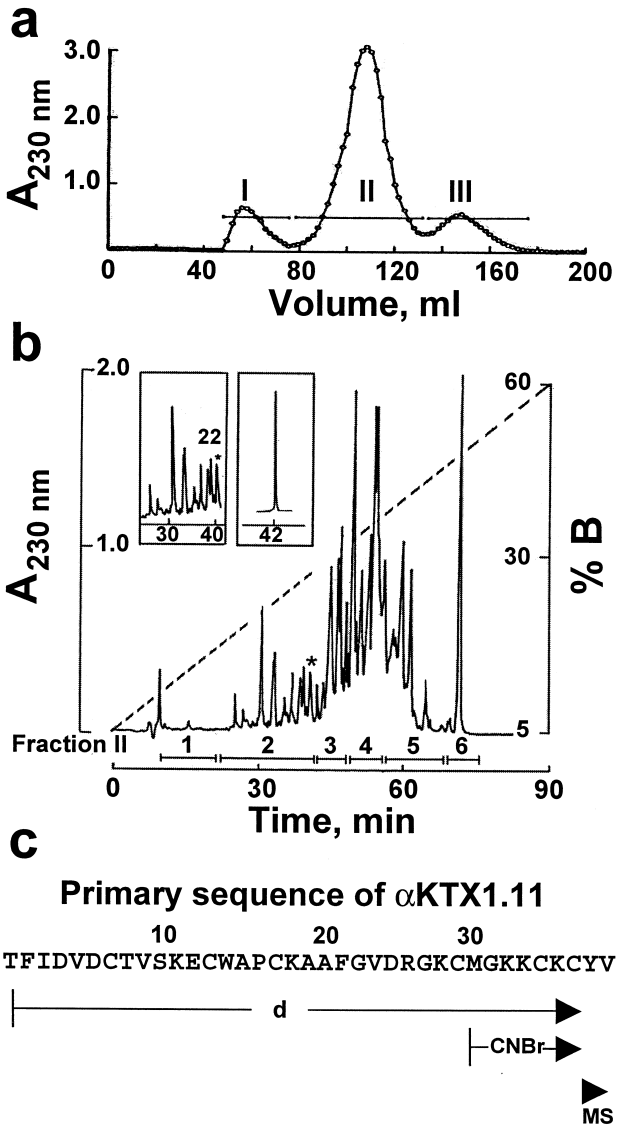

Fig. 1. Purification and sequence of αKTx1.11 (SloTx). a: Three fractions (I–III) were obtained after the soluble *C. noxius* venom (80 mg) was separated in a Sephadex G-50 column using 20 mM ammonium acetate buffer, pH 4.7. b: The active fraction (II) was further separated by HPLC, using a semi-preparative C_{18} reverse-phase column, with a linear gradient of solution A (0.12% trifluoroacetic acid/water) to 60% of solution B (0.10% trifluoroacetic acid/acetonitrile). Left-side inset: Fraction II.2 was run in an analytical C_{18} reverse-phase column with a linear gradient from 5% to 40% solution B in 90 min. Right-side inset: Re-chromatography of component 22 (labeled with asterisk in the left-side inset). Pure peptide corresponds to less than 0.5% of the soluble venom. c: Amino acid sequence obtained by direct sequencing of the native peptide (d), CNBr cleaved peptide, and mass spectrometry analysis (MS). Arrows mark the sequence obtained by each method.

Sequence comparison using BLASTP showed that the purified peptide has a greater similarity with the ChTx sub-family, αKTx1, than to other sub-families of the short-chain αKTx family from scorpion venoms [18]. The new toxin is closely related to limbatustoxin (LbTx; αKTx1.4) [25] with 84% identity, and to iberiotoxin (IbTx; αKTx1.3) with 76% identity. The identity with ChTx (αKTx1.1) was only 54% (Fig. 2a). We decided to classify this new toxin, αKTx1.11,

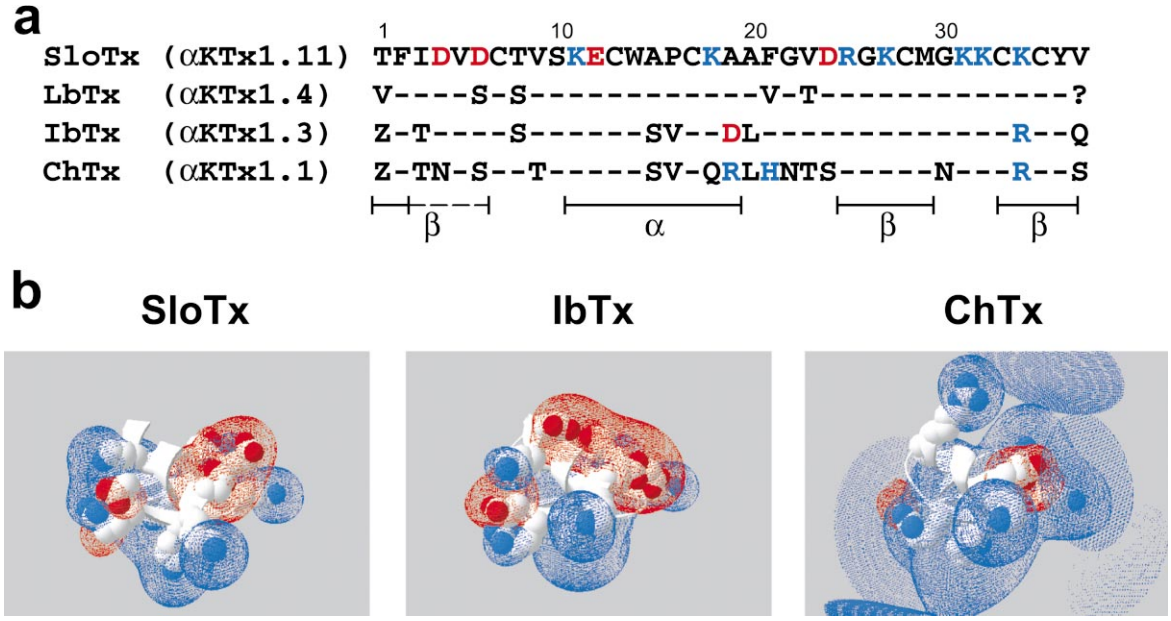

Fig. 2. Molecular characteristics of αKTx1.11 (SloTx). a: Amino acid sequence comparison of SloTx, LbTx, IbTx and ChTx. Toxins were aligned using the Pileup program (Genetics Computer Group). Dashes: Identical residues; question mark: unknown residue. Amino acids forming α-helix and β-strands in IbTx (dashed line) and ChTx are marked [25,31]. b: Predicted electrostatic isopotential of SloTx, IbTx and ChTx. Red surfaces represent negative electrostatic isopotentials at a free energy of −2 *kT*/e; the blue surfaces are for positive isopotentials of +2 *kT*/e. Molecules are oriented such that the bottom part would interact with the pore of K^+ channels [27–29].

according to the international nomenclature proposed recently by Tytgat et al. [18]. Consistent with its sequence similarity to LbTx, IbTx and ChTx, αKTx1.11 is also a potent inhibitor of the mammalian MaxiK channel α subunit (Slo) (see Fig. 3), and thus, was given the common name, SloTx.

Multiple sequence alignment of SloTx with LbTx, IbTx and ChTx shows that the C-terminal region from position 25, including two β-sheets [25], is the most conserved region across the molecules (Fig. 2a). In addition, electrostatic potential analysis, at 120 mM ionic strength, demonstrates that similar to IbTx and ChTx, the conserved C-terminal region of SloTx confers to the molecule a positive electrostatic isopotential that is very close to the molecular surface. For illustrative purposes, Fig. 2b shows the electrostatic isopotentials at zero ionic strength, which makes clear that SloTx has a surface that is positively charged (blue grid). These results are consistent with the fact that SloTx blocks MaxiK channels (see Fig. 3) and the view that the positively charged C-terminal domain is a major component for specific short-range interactions between scorpion toxins and the negatively charged pore region of K^+ channels leading to channel blockade [26–29]. Specific hydrophobic residue–residue interactions between SloTx and MaxiK channels may also contribute to toxin–channel interaction as is the case for ChTx [26]. Interestingly, the N-terminal flanking region of the α-helix and prior to the β-sheet is similar in SloTx and IbTx, but distinct in ChTx (Fig. 2a). This region is situated in the face opposite to the site of toxin–pore interaction [29], and might have implications for the modulation of channel blockade by the MaxiK β subunits (see below).

3.2. *Affinity of αKTx1.11 for the MaxiK channel α subunit*

The two-electrode voltage-clamp technique was used during the toxin isolation procedure to measure the activity of different fractions on the MaxiK α subunit (hSlo) currents. As mentioned before, fraction II and sub-fractions II.2 and II.2.22 all had a blocking effect on the MaxiK currents.

The blocking kinetics of the pure peptide (αKTx1.11, SloTx) was determined in outside-out patches expressing the MaxiK α subunit (hSlo) and under conditions to attain a high channel open probability (84 μM $[Ca^{2+}]i$; +40 mV) [13]. Addition of 100 nM SloTx blocked more than 90% of the current (Fig. 3a), which was completely blocked by 10 mM tetraethylammonium (TEA). Toxin blockade reached steady-state within 15–30 s and was fully reversible (Fig. 3a, wash). Fig. 3d shows the normalized current before (1), after addition of toxin (2), and after washout (3) (arrows mark the addition of toxin and the beginning of washout). The data could be well fitted assuming a bimolecular blocking reaction (continuous line). To increase the accuracy of k_{on} measurements, additional experiments with a lower SloTx concentration (10 nM) were performed. k_{on} was $(3.9 \pm 2.2) \times 10^6$ M^{-1} s^{-1}, k_{off} was $(4.8 \pm 1.7) \times 10^{-3}$ s^{-1}, and K_d was 1.5 ± 0.8 nM ($n = 5$). k_{on} and k_{off} values of SloTx are close to those reported for IbTx, but one order of magnitude smaller than the ones for ChTx [5]. The results suggest that SloTx, similar to IbTx and ChTx, interacts with the MaxiK channel pore-forming α subunit by blocking the pore via a bimolecular reaction.

3.3. *β subunit modulation of the SloTx–MaxiK α subunit interaction*

It is known that co-expression of MaxiK accessory β subunits change the voltage and Ca^{2+} sensitivities, the kinetics, and the pharmacology of the MaxiK channel pore-forming α subunit [11,14]. Thus, we decided to explore whether the smooth muscle β1 subunit [30] or neuronal β4 subunit [5] modify the pattern of SloTx blockade of MaxiK channels. To confirm β subunit expression, voltage–activation curves were obtained in all experiments (insets in panels a,b,c). At the calcium concentration tested (~90 μM), β1 caused a left-

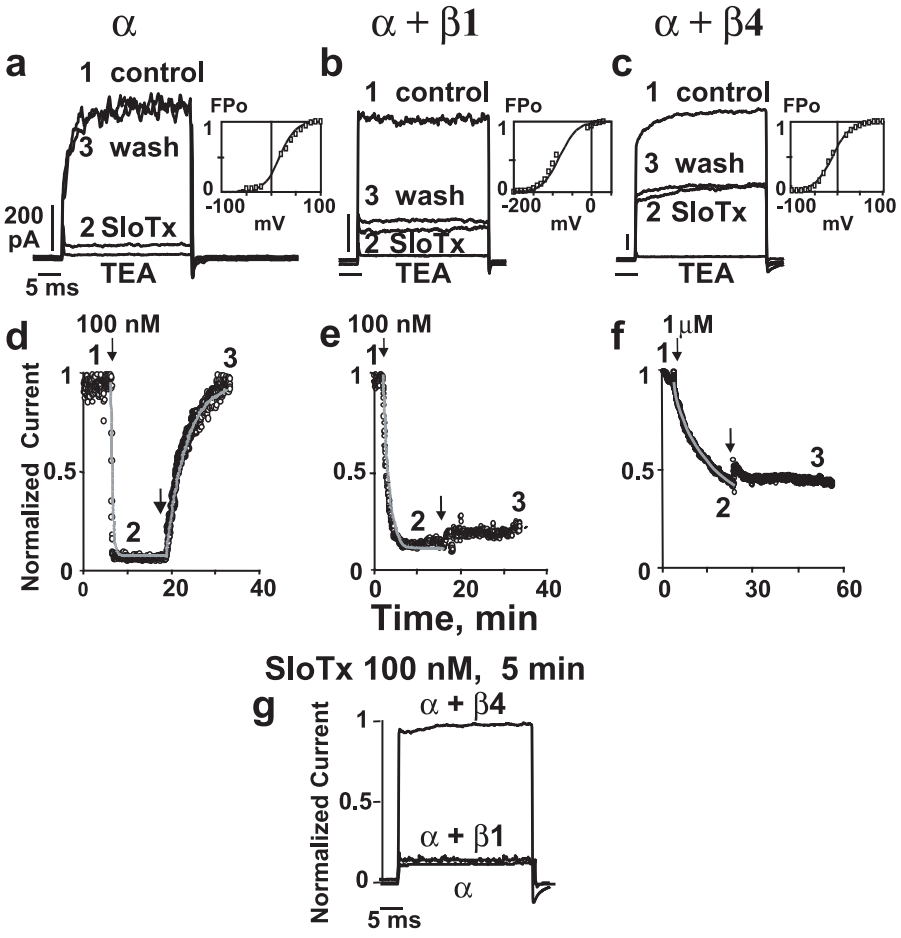

Fig. 3. Blocking properties of αKTx1.11 on MaxiK channels formed by α or α+β complexes. Outside-out patches from *Xenopus* oocytes expressing α (a,d), α+β1 (b,e) and α+β4 (c,f) subunits. Currents were elicited at +40 mV from a holding potential of 0 mV every 2 s. a,b,c: Current traces at specific times during the experiment. Numbers in traces (a,b,c) and in time–course plots (d,e,f) are equivalent. 1: Control; 2: in presence of toxin; 3: after toxin washout. TEA blockade was performed before toxin application. Arrows mark the time of addition of toxin and washout. d,e,f: Steady-state current amplitudes as a function of time. The gray line is the best fit to a bimolecular blocking reaction, which is only an approximation for α+β1 and α+β4 channels. g: Normalized current obtained after 5 min application of 100 nM SloTx to channels formed by α, α+β1 and α+β4. Note that the β4 subunit makes MaxiK channels extremely resistant to SloTx blockade.

ward shift of ~85 mV of the voltage–activation curves, whereas β4 caused a shift of ~39 mV. Half activation potentials were: 22 ± 13 mV ($n = 5$) for the α subunit, −62 ± 8 mV ($n = 5$) for α+β1 subunits and −17 ± 23 mV ($n = 4$) for α+β4 subunits.

Co-expression of the β1 subunit (Fig. 3b,c) slowed down the on-rate of channel blockade by two orders of magnitude to $(5 \pm 2.8) \times 10^4$ M^{-1} s^{-1} ($n = 5$) when compared with the α subunit alone $(3.9 \pm 2.2) \times 10^6$ M^{-1} s^{-1}. In addition, the off-rate was dramatically slowed down making SloTx blockade practically irreversible during the experimental time (Fig. 3e; $n = 5$). Fig. 3b illustrates control records (1), after ~10 min of toxin application (2), and ~15 min following washout (3). It also shows that β1 co-expression does not affect full blockade by 10 mM TEA. Interestingly, if channel blockade was not allowed to reach steady-state, washout induced ~50% of recovery (not shown; $n = 2$), which may be indicative of a second binding step between the channel, the toxin and the extracellular loop of the β1 subunit. Thus, the bimolecular model used to fit the data is only an approximation and K_d values cannot be estimated.

In the case of oocytes co-expressing α+β4 subunits (Fig. 3c,f), the association rate of the toxin was much slower than when β1 was co-expressed. The on-rate was decreased by four orders of magnitude to $(5.9 \pm 1) \times 10^2$ M^{-1} s^{-1} ($n = 4$) when compared to the α subunit alone. On the other hand, the off-rate was even slower, making the toxin dissociation irreversible within the experimental time (~30 min following washout; Fig. 3f). Because of the drastic diminution in the association rate, the toxin concentration was increased to 1 μM to be able to evaluate the on-rate within a reasonable time frame (~25 min; Fig. 3f). Traces in Fig. 3c illustrate the current blockade after ~25 min of toxin application (2), ~30 min following toxin washout (3), and complete blockade with 10 mM TEA. Fig. 3g illustrates the magnitude of α, α+β1 and α+β4 blockade using the same concentration of SloTx (100 nM), 5 min after toxin application. Due to the extreme slow on-rate of SloTx on α+β4 channels, their blockade is imperceptable in this time range, whereas blockade of channels assembled by α+β1 or α subunits was ~90%. In other words, α+β4 channels are extremely resistant to SloTx blockade, but once blocked, the toxin interaction is apparently irreversible.

Experiments using β1 and β4 demonstrate that SloTx binding to the channel is 10 times slower than the interaction of

Table 1
Specificity of αKTx1.11 toxin for MaxiK channels

Channel	≤[SloTx] (nM)	Inhibition
hSlo[a]	200	+
dSlo[a], Kv1.1[b], Herg[b] or IRK2.1[b]	300	−
ShIR[b]	350	−
SK1[a], SK2[a] or SK3[a]	500	−

[a]Outside-out patches and 110 K-methanesulfonate.
[b]Two-electrode voltage-clamp and ND96 or modified ND96.

IbTx and ChTx with the channel when these subunits are present [5]. In fact, 100 nM SloTx is unable to significantly block the channel within 5 min of application in α+β4 channels (Fig. 3g), whereas IbTx or ChTx block ∼20% of the current in this same time frame [5]. Thus, SloTx is a more reliable pharmacological tool than ChTx or IbTx to distinguish channels formed by MaxiK α+β4 complexes.

3.4. Specificity of αKTx1.11 toxin for MaxiK channels

The toxin specificity was assayed in different types of K^+ channels such as the voltage-dependent ShIR (*Shaker* K^+ channel with inactivation removed), Kv1.1, and Herg; the voltage- and calcium-activated hSlo and dSlo; the voltage-independent/calcium-activated SK1, SK2 and SK3; and the voltage-independent IRK2.1. The two-electrode voltage-clamp system was used to study all voltage-dependent K^+ channels and IRK2.1. Outside-out patches were used to study all calcium-dependent K^+ channels. None of these channels showed any type of inhibition when nanomolar concentrations of SloTx were tested (Table 1) and after 10 min of toxin application. The lack of activity of SloTx towards the K^+ channel types examined here mimics the IbTx inactivity on channels other than the MaxiK channels. Thus, IbTx and the new toxin reported here (SloTx, αKTx1.11) are quite specific for MaxiK channels.

In summary, our results open the possibility to use αKTx1.11 for discriminating channels in different tissues that express α, α+β1 or α+β4 channels.

Acknowledgements: This work was supported by grants from Howard Hughes Medical Institute (No. 55000574), CONACyT-Mexico (No. 31691-N) and DGAPA-UNAM (IN216900) to L.P., from NIH (HL-54970) and Human Frontier Science Program Organization to L.T. J.G.V. received a Scholarship from CONACyT-Mexico (No. 62396) and DGEP-UNAM. L.T. is an Established Investigator from the American Heart Association. We thank Genaro Pimienta for helping on the purification of toxin and Cesar Batista for mass spectrometry determinations. We also thank J.P. Adelman, for SK1, SK2 and SK3; R. Joho, for IRK2.1; G. Robertson, for Herg; and M. Montal, for Kv1.1 cDNA.

References

[1] Latorre, R., Oberhauser, A., Labarca, P. and Alvarez, O. (1989) Annu. Rev. Physiol. 51, 385–399.
[2] Knaus, H.G., Folander, K., Garcia-Calvo, M., Garcia, M.L., Kaczorowski, G.J., Smith, M. and Swanson, R. (1994) J. Biol. Chem. 269, 17274–17278.
[3] Wallner, M., Meera, P. and Toro, L. (1999) Proc. Natl. Acad. Sci. USA 96, 4137–4142.
[4] Uebele, V.N., Lagrutta, A., Wade, T., Figueroa, D.J., Liu, Y., McKenna, E., Austin, C.P., Bennett, P.B. and Swanson, R. (2000) J. Biol. Chem. 275, 23211–23218.
[5] Meera, P., Wallner, M. and Toro, L. (2000) Proc. Natl. Acad. Sci. USA 97, 5562–5567.
[6] Wei, A., Solaro, C., Lingle, C. and Salkoff, L. (1994) Neuron 13, 671–681.
[7] Wallner, M., Meera, P. and Toro, L. (1996) Proc. Natl. Acad. Sci. USA 93, 14922–14927.
[8] Meera, P., Wallner, M., Song, M. and Toro, L. (1997) Proc. Natl. Acad. Sci. USA 94, 14066–14071.
[9] Díaz, L., Meera, P., Amigo, J., Stefani, E., Alvarez, O., Toro, L. and Latorre, R. (1998) J. Biol. Chem. 273, 32430–32436.
[10] Garcia, M.L., Hanner, M., Knaus, H.G., Slaughter, R. and Kaczorowski, G.J. (1999) Methods Enzymol. 294, 624–639.
[11] Dworetzky, S.I., Boissard, C.G., Lum-Ragan, J.T., McKay, M.C., Post-Munson, D.J., Trojnacki, J.T., Chang, C.P. and Gribkoff, V.K. (1996) J. Neurosci. 16, 4543–4550.
[12] McManus, O.B., Helms, L.M., Pallanck, L., Ganetzky, B., Swanson, R. and Leonard, R.J. (1995) Neuron 14, 645–650.
[13] Meera, P., Wallner, M., Jiang, Z. and Toro, L. (1996) FEBS Lett. 382, 84–88.
[14] Meera, P., Wallner, M. and Toro, L. (2001) Molecular biology of Ca^{2+}-activated K^+ channels, in: Potassium Channels in Cardiovascular Biology (Archer, S.L. and Rusch, N.J., Eds.), pp. 49–70, Kluwer Academic/Plenum Publishers, New York.
[15] Brenner, R., Jegla, T.J., Wickenden, A., Liu, Y. and Aldrich, R.W. (2000) J. Biol. Chem. 275, 6453–6461.
[16] Possani, L.D., Becerril, B., Delepierre, M. and Tytgat, J. (1999) Eur. J. Biochem. 264, 287–300.
[17] Miller, C. (1995) Neuron 15, 5–10.
[18] Tytgat, J., Chandy, K.G., Garcia, M.L., Gutman, G.A., Martin-Eauclaire, M.F., van der Walt, J.J. and Possani, L.D. (1999) Trends Pharmacol. Sci. 20, 444–447.
[19] Ménez, A., Bontems, F., Roumestand, C., Gilquin, B. and Toma, F. (1992) Proc. R. Soc. Edinburgh 99B, 83–103.
[20] Zamudio, F.Z., Conde, R., Arevalo, C., Becerril, B., Martin, B.M., Valdivia, H.H. and Possani, L.D. (1997) J. Biol. Chem. 272, 11886–11894.
[21] Conde, R., Zamudio, F.Z., Becerril, B. and Possani, L.D. (1999) FEBS Lett. 460, 447–450.
[22] Zhou, W., Merrick, B.A., Khaledi, M.G. and Tomer, K.B. (2000) J. Am. Soc. Mass Spectrom. 11, 273–282.
[23] Guex, N., Diemand, A. and Peitsch, M.C. (1999) Trends Biochem. Sci. 24, 364–367.
[24] Schoenmakers, T.J., Visser, G.J., Flik, G. and Theuvenet, A.P. (1992) Biotechniques 12, 870–879.
[25] Giangiacomo, K.M., Gabriel, J., Fremont, V. and Mullmann, T.J. (1999) Perspect. Drug Discov. Des. 15/16, 167–186.
[26] Park, C.S. and Miller, C. (1992) Biochemistry 31, 7749–7755.
[27] Stampe, P., Kolmakova-Partensky, L. and Miller, C. (1994) Biochemistry 33, 443–450.
[28] Mullmann, T.J., Munujos, P., Garcia, M.L. and Giangiacomo, K.M. (1999) Biochemistry 38, 2395–2402.
[29] Cui, M., Shen, J., Briggs, J.M., Luo, X., Tan, X., Jiang, H., Chen, K. and Ji, R. (2001) Biophys. J. 80, 1659–1669.
[30] Jiang, Z., Wallner, M., Meera, P. and Toro, L. (1999) Genomics 55, 57–67.
[31] Johnson, B.A. and Sugg, E.E. (1992) Biochemistry 31, 8151–8159.